

This is the accepted manuscript made available via CHORUS. The article has been published as:

# In-beam $\gamma$ -ray spectroscopy studies of medium-spin states in the odd-odd nucleus $^{186}\text{Re}$

D. A. Matters *et al.*

Phys. Rev. C **96**, 014318 — Published 27 July 2017

DOI: [10.1103/PhysRevC.96.014318](https://doi.org/10.1103/PhysRevC.96.014318)

# In-beam $\gamma$ -ray spectroscopy studies of medium-spin states in the odd-odd nucleus $^{186}\text{Re}$

D. A. Matters,<sup>1,\*</sup> F. G. Kondev,<sup>2</sup> N. Aoi,<sup>3</sup> Y. Ayyad,<sup>4,†</sup> A. P. Byrne,<sup>5</sup> M. P. Carpenter,<sup>6</sup>  
J. J. Carroll,<sup>7</sup> C. J. Chiara,<sup>8</sup> P. M. Davidson,<sup>5</sup> G. D. Dracoulis,<sup>5,‡</sup> Y. D. Fang,<sup>3</sup> C. R. Hoffman,<sup>6</sup>  
R. O. Hughes,<sup>5</sup> E. Ideguchi,<sup>3</sup> R. V. F. Janssens,<sup>6</sup> S. Kanaya,<sup>9</sup> B. P. Kay,<sup>6</sup> T. Kibédi,<sup>5</sup>  
G. J. Lane,<sup>5</sup> T. Lauritsen,<sup>6</sup> J. W. McClory,<sup>1</sup> P. Nieminen,<sup>5</sup> S. Noji,<sup>3,§</sup> A. Odahara,<sup>9</sup> H. J. Ong,<sup>3</sup>  
A. E. Stuchbery,<sup>5</sup> D. T. Tran,<sup>3</sup> H. Watanabe,<sup>10,11,12</sup> A. N. Wilson,<sup>5</sup> Y. Yamamoto,<sup>3</sup> and S. Zhu<sup>6</sup>

<sup>1</sup>*Department of Engineering Physics, Air Force Institute of Technology, Wright-Patterson AFB, Ohio 45433, USA*

<sup>2</sup>*Nuclear Engineering Division, Argonne National Laboratory, Argonne, Illinois 60439, USA*

<sup>3</sup>*Research Center for Nuclear Physics, Osaka University, Osaka 567-0047, Japan*

<sup>4</sup>*National Superconducting Cyclotron Laboratory, Michigan State University, East Lansing, Michigan 48824, USA*

<sup>5</sup>*Department of Nuclear Physics, R.S.P.E., Australian National University, Canberra ACT 2615, Australia*

<sup>6</sup>*Physics Division, Argonne National Laboratory, Argonne, Illinois 60439, USA*

<sup>7</sup>*U.S. Army Research Laboratory, Adelphi, Maryland 20783, USA*

<sup>8</sup>*Oak Ridge Associated Universities Fellowship Program,*

*U.S. Army Research Laboratory, Adelphi, Maryland 20783, USA*

<sup>9</sup>*Department of Physics, Osaka University, Osaka 560-0043, Japan*

<sup>10</sup>*RIKEN Nishina Center, Wako, Saitama 351-0198, Japan*

<sup>11</sup>*School of Physics and Nuclear Energy Engineering, Beihang University, Beijing 100191, China*

<sup>12</sup>*International Research Center for Nuclei and Particles in the Cosmos, Beihang University, Beijing 100191, China*

Excited states in  $^{186}\text{Re}$  with spins up to  $J = 12\hbar$  were investigated in two separate experiments using  $^{186}\text{W}(\text{d},\text{n})$  reactions at beam energies of 12.5 MeV and 14.5 MeV. Two- and three-fold  $\gamma$ -ray coincidence data were collected using the CAESAR and CAGRA spectrometers, respectively, each composed of Compton-suppressed HPGe detectors. Analysis of the data revealed rotational bands built on several two-quasiparticle intrinsic states, including a long-lived  $K^\pi = (8^+)$  isomer. Configuration assignments were supported by an analysis of in-band properties, such as  $|g_K - g_R|$  values. The excitation energies of the observed intrinsic states were compared with results from multi-quasiparticle blocking calculations, based on the Lipkin-Nogami pairing approach, that included contributions from the residual proton-neutron interactions.

## I. INTRODUCTION

The odd-odd nucleus  $^{186}_{75}\text{Re}$  ( $N = 111$ ) is located near the line of stability in the upper part of the deformed, rare-earth region. There is a continuing interest in studying properties of nuclei in this region, especially beyond the deformed sub-shell gap at  $N = 106$  ( $\beta_2 \sim 0.25$ ), since their deformation is expected to decrease rapidly with neutron number. The dependence of deformation on  $N$  could lead to changes in the single-particle structure of these nuclei. It could also have implications for the frequency of high- $K$ , multi-quasiparticle isomers, which are found along the yrast lines of axially-symmetric, well-deformed nuclei in this region [1, 2], owing to deviations from axial symmetry.

There is little experimental information available about the high-spin structure of  $^{186}\text{Re}$ . This is due in part to the lack of heavy-ion fusion-evaporation reactions with stable beams and targets that can preferentially populate high-spin states in this nucleus. A very long-lived ( $T_{1/2} \approx 2.0 \times 10^5$  y)  $K^\pi = (8^+)$  isomer, designated here as  $^{186m}\text{Re}$ , is known to exist at a relatively low excitation energy of  $\sim 150$  keV [3, 4]. From an experimental point of view, this isomer represents a challenge for  $\gamma$ -ray spectroscopy studies, since the long half-life precludes practical measurements of  $\gamma$ -ray coincidence relationships across the isomer. Consequently, data on levels and  $\gamma$  rays above the isomer are to a large extent unavailable.

Interest in the level structures above  $^{186m}\text{Re}$  is motivated by the fact that the isomer could contribute to the production of  $^{187}\text{Re}$  in  $s$ -process nucleosynthesis. In this context, accurate cross sections for the production of  $^{186m}\text{Re}$  via slow-neutron capture on  $^{185}\text{Re}$  are important for reducing the nuclear physics uncertainties in the  $^{187}\text{Re}/^{187}\text{Os}$  cosmochronometer [5]. Previous measurements have suggested that  $^{186m}\text{Re}$  contributes negligibly to the chronometer uncertainty [5], but they were performed using the activation technique, which is sensitive to the imprecisely-known half-life of the isomer. An al-

\* david.a.matters.mil@mail.mil; Present address: Defense Threat Reduction Agency, Fort Belvoir, Virginia 22060, USA.

† Present address: Lawrence Berkeley National Laboratory, Berkeley, California 94720, USA.

‡ Deceased.

§ Present address: National Superconducting Cyclotron Laboratory, Michigan State University, East Lansing, Michigan 48824, USA.

ternative approach to determine the  $^{185}\text{Re}(n,\gamma)^{186m}\text{Re}$  cross section, which is independent of the isomer half-life, is to apply statistical modeling to the observed capture- $\gamma$  cascades feeding the isomer. This procedure, recently demonstrated by Matters *et al.* [6], relies on detailed knowledge of level structures above the isomer.

Previously, spectroscopy studies of  $^{186}\text{Re}$  were carried out by Lanier *et al.* [7] using (d,t), (d,p), (n, $\gamma$ ), and (n, $e^-$ ) reactions. While a large number of  $\gamma$  rays were observed in singles measurements using high-resolution, bent-crystal and Ge(Li) spectrometers, only a few of these were placed in the level scheme. Glatz [8], using the (n, $\gamma$ ) reaction and the  $\gamma$ - $\gamma$  coincidence technique with one Ge(Li) and one NaI(Tl) detector, proposed several  $\gamma$  rays above a  $K^\pi = 6^-$  state at  $E_x \approx 186$  keV, which was assessed to be an isomeric state in Ref. [7]. Wheldon *et al.* [9], using the (p,d) reaction and a high-resolution magnetic spectrograph, observed a number of two-quasiparticle excited states in  $^{186}\text{Re}$ . However, because of a lack of angular distribution data, the spin, parity, and configuration assignments were based on model calculations rather than on experimental data. Recently, Matters *et al.* [10] used the (n,2n) reaction to reveal several new levels and  $\gamma$ -ray transitions assessed as feeding the long-lived,  $K^\pi = (8^+)$  isomer. These authors have also studied low-spin states using the  $^{185}\text{Re}(n,\gamma)$  reaction [6].

In the present work, we report for the first time on  $\gamma$ -ray spectroscopy studies using the  $^{186}\text{W}(d,2n)$  reaction in conjunction with high-efficiency, Compton-suppressed HPGe arrays.

## II. EXPERIMENTS

The experimental data described in the present work were collected in two separate experiments, both of which used (d,2n) reactions and a 6 mg/cm<sup>2</sup>-thick target enriched to 80% in  $^{186}\text{W}$ .

In the first experiment, the 14UD Pelletron accelerator at the Australian National University (ANU) was used to produce a deuteron beam with an intensity of  $\sim 0.5$  pA at energies ranging between 12 MeV and 18 MeV. The excitation function for the  $^{186}\text{W}(d,2n)$  reaction was mapped in this energy range by collecting and analyzing singles  $\gamma$ -ray spectra. Two-fold  $\gamma$ - $\gamma$  coincidence measurements were subsequently performed over a two-day period at beam energies of 12.5 MeV and 14.5 MeV. The former was chosen close to the fusion barrier in order to suppress other neutron-evaporation reaction channels (particularly the 3n one leading to  $^{185}\text{Re}$ ), while the latter was selected to maximize production of the  $^{186m}\text{Re}$  isomer. The CAESAR  $\gamma$ -ray detector array, which comprised nine Compton-suppressed HPGe detectors and two unsuppressed planar low-energy photon spectrometers (LEPS), was used for these measurements.

The second experiment was performed using the Clover

Array Gamma-ray spectrometer at RCNP/RIBF for Advanced research (CAGRA) at the Research Center for Nuclear Physics (RCNP) at Osaka University. This array was developed jointly between the U.S., Japan, and China, and consisted of 16 Clover-type HPGe detectors, Compton-suppressed using bismuth-germanate shields. The detectors were arranged in such a way that four were positioned at  $45^\circ$  and  $135^\circ$  relative to the incident beam direction, and eight were oriented at  $90^\circ$ . The RCNP AVF cyclotron provided a 14.5-MeV deuteron beam with an average current of  $\sim 2.0$  pA. Two-fold and higher  $\gamma$ -ray coincidence data were continuously collected over seven days.

The energy and efficiency calibrations in both experiments were carried out using standard  $^{133}\text{Ba}$  and  $^{152}\text{Eu}$  radioactive sources.

## III. ANALYSIS AND RESULTS

The  $\gamma$ -ray coincidence data collected using the CAGRA and CAESAR spectrometers were sorted offline into three-dimensional ( $E_\gamma$ - $E_\gamma$ - $E_\gamma$ ) and symmetrized, two-dimensional ( $E_\gamma$ - $E_\gamma$ ) histograms, respectively. Data analyses were performed using the LEVIT8R and ESCL8R programs from the RADWARE software package [11].

The partial level scheme of  $^{186}\text{Re}$  determined in the present work is given in Fig. 1. It was constructed on the basis of observed  $\gamma$ -ray coincidence relationships in the two-fold data collected with the CAESAR array and confirmed via a parallel analysis of the three-fold data measured with the CAGRA spectrometer.

A  $\gamma$ -ray coincidence spectrum produced by gating on the 186.1-keV transition is found in Fig. 2(a). From earlier work, it was determined that the 141.1-keV  $\gamma$  ray has  $M1$  character [7], and this  $\gamma$  ray was proposed to depopulate an intrinsic  $K^\pi = 4^+$  state [8, 10]. Matters *et al.* [6] revised the assignment to  $J^\pi = 6^+$  on the basis of a statistical analysis of the  $^{185}\text{Re}(n,\gamma)^{186}\text{Re}$   $\gamma$ -ray cascade intensities. Here, the 141.1-keV  $\gamma$  ray is assigned as the first cascade transition within the  $K^\pi = 5^+$  band, which is established for the first time in the present study. This was aided by the observation of the 327.5-keV,  $7^+ \rightarrow 5^+$  crossover transition, as shown in Fig. 1. The 144.0-keV and 150.3-keV  $\gamma$  rays were found to depopulate in parallel the  $K^\pi = 5^+$  band head. The newly observed 150.3-keV transition was in prompt ( $\pm 40$  ns) coincidence with the 74.7-keV one, known to depopulate the 174.1-keV level [7, 8]. This relationship permitted determination of a precise value of 324.4 keV for the excitation energy of the  $K^\pi = 5^+$  band head, which was known previously as  $\sim 330$  keV [4, 6, 7, 10]. The 144.0-keV  $\gamma$  ray was observed to terminate at the 180.4-keV level, implying that the latter is a long-lived isomeric state. Lanier *et al.* [7] associated this level with the  $T_{1/2} = 70(1)$   $\mu\text{s}$  isomer in  $^{186}\text{Re}$  proposed by Brandi *et al.* [13], which was not assigned to a specific state, nor was its configuration revealed in the

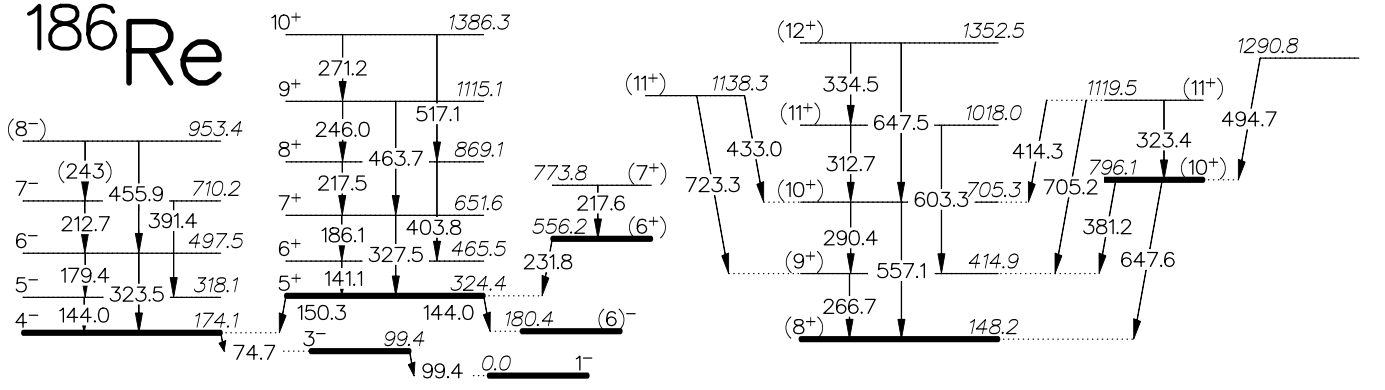


Figure 1. Partial  $^{186}\text{Re}$  level scheme from the present work, with measured  $\gamma$ -ray energies in plain text and deduced level energies in italics. The intrinsic levels are indicated with thick lines. For  $\gamma$  rays with  $E_\gamma > 100$  keV, the uncertainty in the transition energies is  $\pm 0.5$  keV. For those with  $E_\gamma < 100$  keV, which were measured with the LEPS detectors, the uncertainty is  $\pm 0.2$  keV. Tentative  $\gamma$ -ray transitions and  $J^\pi$  assignments are identified with parentheses. The  $J^\pi = 3^-$  level at 99.4 keV is shown to illustrate the decay path to the  $J^\pi = 1^-$  ground state. The excitation energy of 148.2 keV for the  $K^\pi = (8^+)$  isomer is from Ref. [10].

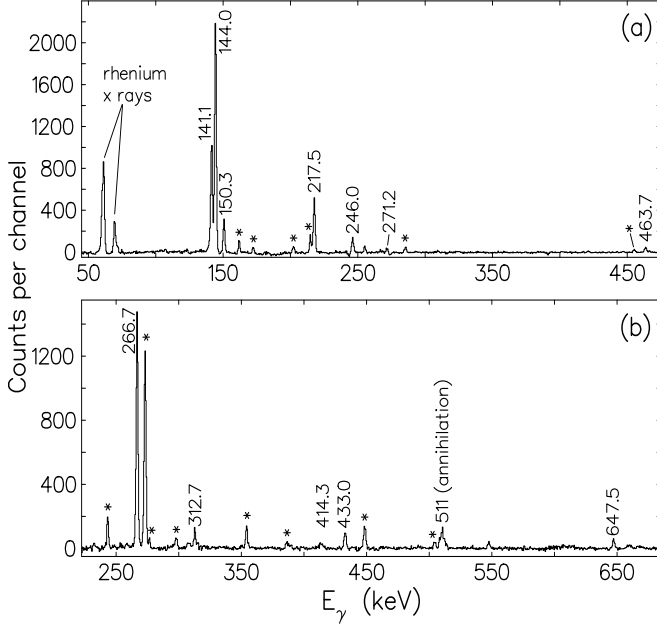


Figure 2. Representative  $\gamma$ -ray coincidence spectra from data collected with the CAESAR (ANU) spectrometer, showing (a) a gate on the 186.1-keV  $\gamma$  ray in the  $E_d = 12.5$  MeV data, and (b) a gate on the 290.4-keV  $\gamma$  ray in the  $E_d = 14.5$  MeV data. Contaminant  $\gamma$ -ray peaks are identified with asterisks (\*).

latter work.

The  $K^\pi = 5^+$  and  $(6)^-$  assignments for the 324.4- and 180.4-keV levels, respectively, were supported by establishing  $E1$  multiplicities for the 150.3- and 144.0-keV transitions. These multiplicities were deduced from balancing the total intensities of the transitions into and out

Table I. Efficiency-corrected relative  $\gamma$ -ray intensities ( $I_\gamma$ ) for the 141.1-, 144.0-, and 150.3-keV  $\gamma$  rays, measured from the ANU data using a spectrum produced by gating on the 186.1-keV  $\gamma$  ray. The total internal conversion coefficients ( $\alpha_T$ ) were calculated using the BRICC code [12], assuming the indicated multipolarity ( $M\lambda$ ), with a nominal uncertainty of 1.4%.

$E_\gamma$ [keV]	$I_\gamma$ [arb.]	$M\lambda$	$\alpha_T$	$I_\gamma \times (1 + \alpha_T)$ [arb.]
141.1(5)	1.10(6)	$M1 + E2$	1.6(3) <sup>a</sup>	2.9(4)
144.0(5)	2.43(12)	<b><math>E1</math></b>	<b>0.150(2)</b>	<b>2.79(14)</b>
		$M1$	1.826(26)	6.9(3)
		$E2$	1.015(14)	4.90(24)
150.3(5)	0.32(2)	<b><math>E1</math></b>	<b>0.134(2)</b>	<b>0.36(2)</b>
		$M1$	1.617(23)	0.84(5)
		$E2$	0.869(12)	0.60(4)

<sup>a</sup>Calculated using a mixing ratio of  $\delta = 0.9(+9/-5)$  [4], deduced from  $\alpha_K(\text{exp}) = 1.1(4)$  [7].

of the 324.4-keV level, as summarized in Table I. Relative intensities for the 141.1-, 144.0-, and 150.3-keV  $\gamma$  rays were obtained by fitting the spectrum from the ANU data produced by gating on the 186.1-keV  $\gamma$  ray. The time difference between two coincident  $\gamma$  rays was chosen within  $\pm 170$  ns, in order to compensate for the known short lifetime of  $T_{1/2} = 17.4(7)$  ns for the 324.4-keV level [8]. It is worth noting that the  $K$ -shell conversion coefficients for the 144.152-keV and 150.500-keV  $\gamma$  rays measured by Lanier *et al.* [7], which were tabulated, but not placed in the level scheme in their work, are also consistent with the  $E1$  multiplicities proposed above.

The  $K^\pi = 4^-$  intrinsic state at 174.1 keV was established previously [7, 8, 14], as were the  $J^\pi = 5^-$  and  $6^-$  in-band levels [8, 14]. In the present work, the band is extended up to  $J^\pi = (8^-)$ . Wheldon *et al.* [9] also reported levels at 710.2(15) keV and 953.3(20) keV, but they were not placed in the  $K^\pi = 4^-$  band, as proposed here. The previously known  $K^\pi = (6^+)$  state [8, 14] is also confirmed in the present work, and the 217.6-keV  $\gamma$  ray is interpreted as the first in-band cascade transition. The spin assignments are supported by the measured  $K$ -shell electron conversion coefficients of  $\alpha_K(\text{exp}) = 0.35(6)$  and  $0.7(3)$  for the 232.100-keV and 217.91-keV  $\gamma$  rays, respectively, from Ref. [7], both consistent with  $M1$  multipolarity.

A rotational band built on the  $K^\pi = (8^+)$  isomer was established for the first time in the present work, together with other excited structures above the isomer, as indicated in Fig. 1. The assignment to  $^{186}\text{Re}$  was based on coincidences with Re x rays, knowledge of the level structures in the neighboring  $^{184}\text{Re}$  and  $^{185}\text{Re}$  nuclei, and the relative yields deduced from spectra produced by gating on the in-band transition in the 12.5- and 14.5-MeV coincidence data. A  $\gamma$ -ray spectrum from the ANU  $\gamma$ - $\gamma$  coincidence data produced by gating on the 290.4-keV  $\gamma$  ray is given in Fig. 2(b). The 266.7-, 381.2-, and 647.6-keV transitions were reported in the  $^{187}\text{Re}(n, 2n)$  study [10]. However, the latter two were assigned in the present work to depopulate the 796.1-keV level, rather than as being associated with the  $K^\pi = (8^+)$  band structure. From a plot of the excitation energy of the band levels as a function of the spin (see Fig. 3) one can notice that the presently-established band is very similar to the one built upon the same configuration in the neighboring odd-odd  $^{184}\text{Re}$  nucleus [14]. However, if one assumes that the  $K^\pi = (8^+)$  band includes the 381.2-keV  $\gamma$  ray as the  $10^+ \rightarrow 9^+$  in-band transition, as proposed in Ref. [10], then the band deviates significantly from that in  $^{184}\text{Re}$ . Hence, the placement of the 796.1-keV state as belonging to a separate structure appears warranted.

The spin and parity of the 796.1-keV level is most likely  $10^+$ . The alternative spin of  $J = 9$  is unlikely, since then the depopulating 381.2- and 647.6-keV transitions could both be of dipole character. This would result in a branching ratio of  $I_\gamma(647.6 \text{ keV})/I_\gamma(381.2 \text{ keV}) \approx 44$  that differs significantly from the experimentally-measured value of  $I_\gamma(647.6 \text{ keV})/I_\gamma(381.2 \text{ keV}) = 2.0(2)$ .

#### IV. DISCUSSION

Configuration assignments for the observed structures were motivated by comparisons of the experimental intrinsic level energies with results of multi-quasiparticle, Nilsson-type calculations and by the analysis of measured and calculated  $|g_K - g_R|$  values for each rotational band observed.

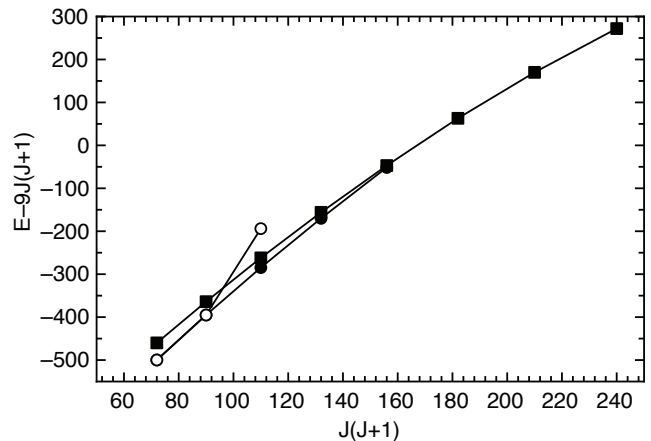


Figure 3. A plot of the excitation energies of the  $K^\pi = (8^+)$  band levels minus a rigid-rotor reference versus  $J(J+1)$ . The filled circles and squares correspond to the  $K^\pi = (8^+)$  bands in  $^{186}\text{Re}$  (present work) and  $^{184}\text{Re}$  [14], respectively. The open circles indicate the alternative interpretation, in which the first two  $K^\pi = (8^+)$  in-band transitions in  $^{186}\text{Re}$  are assumed to have energies of 266.7 keV and 381.2 keV (see text).

#### A. Multi-quasiparticle blocking calculations

In general, the intrinsic two-quasiparticle states of  $^{186}\text{Re}$  can be described by the coupling of the proton  $5/2^+[402]$  or  $9/2^-[514]$  orbitals to the  $1/2^-[510]$ ,  $3/2^-[512]$ ,  $7/2^-[503]$ , or  $11/2^+[615]$  neutron orbitals. Predictions of the excitation energy, spin, and parity for the intrinsic states in  $^{186}\text{Re}$  were obtained using multi-quasiparticle blocking calculations, identical to those reported in Ref. [15]. Specifically, the set of single-particle orbitals originating from the  $N = 4, 5$ , and  $6$  oscillator shells were taken from the Nilsson model with parameters  $\kappa$  and  $\mu$  from Ref. [16], and equilibrium deformation parameters  $\varepsilon_2 = 0.242$  and  $\varepsilon_4 = 0.052$  from Ref. [17]. The states close to the proton and neutron Fermi surfaces were adjusted to approximately reproduce the average experimental one-quasiparticle energies in  $^{185}\text{Re}$  and  $^{187}\text{Re}$  (for the protons) and  $^{185}\text{W}$  and  $^{187}\text{Os}$  (for the neutrons) [4, 18]. The pairing correlations were treated using the Lipkin-Nogami prescription with fixed strengths of  $G_\pi = 20.8/A$  MeV and  $G_\nu = 18.0/A$  MeV, chosen so that the proton and neutron ground-state pairing gaps fit on average the odd-even mass differences from the known atomic mass data [19]. The predicted energies of the multi-quasiparticle states were subsequently corrected for residual interactions using the prescription of Ref. [20] and the Gallagher-Moszkowski splitting energies of Ref. [21]. The calculated excitation energies for a number of intrinsic states in  $^{186}\text{Re}$ , together with the experimental observations, are summarized in Table II and displayed graphically in Figure 4. In general, the theoretical and experimental energies agree to within 100 keV, but there are some exceptions. For example, the  $K^\pi = 6^+$ ,  $\pi 9/2^-[514] \otimes \nu 3/2^-[512]$  state is predicted at 441 keV,



while the experimental one is proposed at 556.2 keV. By the same token, the four-quasiparticle  $K^\pi = 10^+$ ,  $\pi 5/2^+[402] \otimes \nu(1/2^-[510], 3/2^-[512], 11/2^+[615])$  state is predicted at 976 keV, but the observed level at 796.1 keV is proposed as a possible candidate.

Table II. Predicted ( $E_{\text{calc}}$ ) and experimental ( $E_{\text{exp}}$ ) multi-quasiparticle states in  $^{186}\text{Re}$ . Calculated intrinsic-state energies include the modeled two-quasiparticle energies ( $E_{\text{qp}}$ ) combined with the residual-interaction corrections ( $E_{\text{res}}$ ).

$K^\pi$	Configuration		$E_{\text{qp}}$	$E_{\text{res}}$	$E_{\text{calc}}^a$	$E_{\text{exp}}$
	$\pi$	$\nu$	[keV]			
$1^-$	$5/2^+[402]$	$3/2^-[512]$	0	-78	0	0.0
$3^-$	$5/2^+[402]$	$1/2^-[510]$	26	-55	49	99.4
$8^+$	$5/2^+[402]$	$11/2^+[615]$	201	-125	154	148.2
$4^-$	$5/2^+[402]$	$3/2^-[512]$	0	78	156	174.1
$6^-$	$5/2^+[402]$	$7/2^-[503]$	245	-97	226	180.4
$2^-$	$5/2^+[402]$	$1/2^-[510]$	26	55	159	210.7 <sup>b</sup>
$3^+$	$5/2^+[402]$	$11/2^+[615]$	201	125	404	314.0 <sup>b</sup>
$1^-$	$5/2^+[402]$	$7/2^-[503]$	245	97	420	316.5 <sup>b</sup>
$5^+$	$9/2^-[514]$	$1/2^-[510]$	312	-72	318	324.4
$3^+$	$9/2^-[514]$	$3/2^-[512]$	286	-77	287	351.2 <sup>b</sup>
$10^-$	$9/2^-[514]$	$11/2^+[615]$	487	-143	422	
$4^+$	$9/2^-[514]$	$1/2^-[510]$	312	72	462	425.8 <sup>b</sup>
$8^+$	$9/2^-[514]$	$7/2^-[503]$	531	-107	502	
$6^+$	$9/2^-[514]$	$3/2^-[512]$	286	77	441	556.2
$2^-$	$5/2^+[402]$	$9/2^-[505]$	784	-75	787	577.7 <sup>b</sup>
$1^+$	$9/2^-[514]$	$7/2^-[503]$	531	107	716	601.6 <sup>b</sup>
$1^-$	$9/2^-[514]$	$11/2^+[615]$	487	143	708	761.4 <sup>b</sup>
$10^+$	$5/2^+[402]$	$1/2^-, 3/2^-, 11/2^{+c}$	1096	-198	976	796.1
$7^-$	$5/2^+[402]$	$9/2^-[505]$	784	75	937	
$9^+$	$9/2^-[514]$	$9/2^-[505]$	1070	107	1255	
$10^+$	$5/2^+[402]$	$13/2^+[606]$	2552	-125	2427	

<sup>a</sup>Calculated energies relative to the  $K^\pi = 1^-$  ground state,  $E_{\text{qp}}(1^-) + E_{\text{res}}(1^-) = -78$  keV.

<sup>b</sup>Abbreviated value from the ENSDF evaluation of Baglin [4].

<sup>c</sup> $1/2^-, 3/2^-, 11/2^+$ :  $1/2^-[510], 3/2^-[512], 11/2^+[615]$ .

## B. Branching ratios and $|g_K - g_R|$ analysis

In cases where rotational bands were observed, their properties were used to assist with proposing configurations. For example, the in-band branching ratio  $\lambda = I_\gamma(J \rightarrow J-2)/I_\gamma(J \rightarrow J-1)$  can be used in the rotational model [22] to deduce the mixing ratio  $\delta$  and  $|g_K - g_R|$

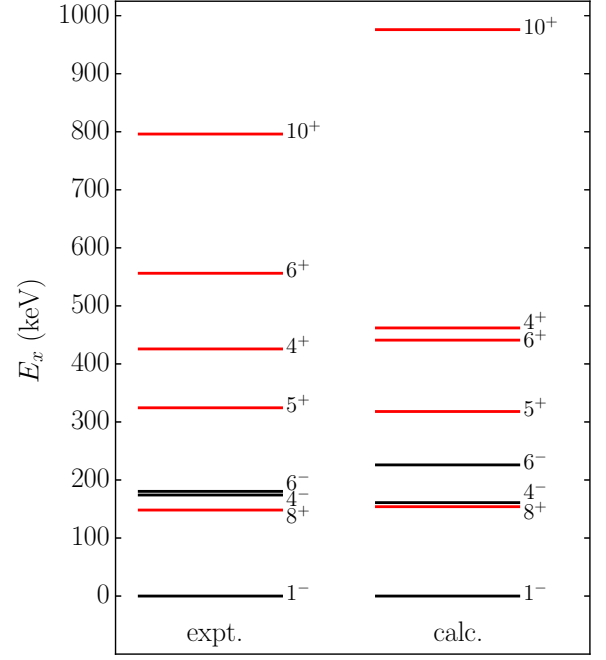


Figure 4. Comparison between experimental level energies (expt.) and results from the multi-quasiparticle blocking calculations (calc.) for the ground state and medium-spin ( $K \geq 4$ ) intrinsic states, with excitation energies  $E_x$  and  $K^\pi$  assignments as listed in Table II. Negative-parity states are identified with black lines, and positive-parity states are in red.

value using the formulae:

$$\frac{\delta^2}{1 + \delta^2} = \frac{2K^2(2J-1)\lambda}{(J-K-1)(J+K-1)(J+1)} \left( \frac{E_1}{E_2} \right)^5 \quad (1)$$

and

$$\left| \frac{g_K - g_R}{Q_0} \right| = 0.933 \frac{E_1}{\delta \sqrt{J^2 - 1}}, \quad (2)$$

where  $Q_0$  is the intrinsic quadrupole moment,  $g_K$  and  $g_R$  are the intrinsic and collective gyromagnetic ratios, respectively, and  $E_1$  and  $E_2$  are the  $\Delta J = 1$  and  $\Delta J = 2$  in-band transition energies in MeV. The experimental  $|g_K - g_R|_{\text{exp}}$  values for the  $K^\pi = 4^-, 5^+$ , and  $(8^+)$  bands are given in Table III. The value  $Q_0 = 6.18(6)$  eb, deduced from the measured spectroscopic quadrupole moment of  $Q = +0.618(6)$  eb [23] for the  $K^\pi = 1^-$  ground state, was used. This assumption is reasonable, since the quadrupole moments are known to be essentially constant with excitation energy for nuclei in this region [24].

Theoretical predictions using the Woods-Saxon potential with a universal parametrization [25] and deformation parameters  $\beta_2 = 0.221$ ,  $\beta_4 = -0.094$ , and  $\beta_6 = 0.010$  [26], together with  $g_R = 0.28$ , are also given in Table III.

Table III. Gamma-ray energies  $E_2$  and  $E_1$ , and branching ratios  $\lambda$ , for  $\Delta J = 2$  and  $\Delta J = 1$  in-band transitions used to determine the experimental  $|g_K - g_R|_{\text{exp}}$  values for the observed rotational bands in  $^{186}\text{Re}$ . Calculated  $|g_K - g_R|_{\text{calc}}$  values are also included for comparison.

$K^\pi$ [ $\hbar$ ]	$J^\pi$ [ $\hbar$ ]	$E_1$ [keV]	$E_2$ [keV]	$\lambda$	$ g_K - g_R _{\text{exp}}$	$ g_K - g_R _{\text{calc}}$
$4^-$	$6^-$	179.4(5)	323.5(5)	0.13(1)	0.88(4)	0.93
$5^+$	$7^+$	186.1(5)	327.5(5)	0.09(1)	0.76(4)	0.73
	$8^+$	217.5(5)	403.8(5)	0.22(2)	0.83(4)	
	$9^+$	246.0(5)	463.7(5)	0.51(4)	0.72(3)	
	$10^+$	271.2(5)	517.1(5)	0.69(6)	0.75(4)	
Weighted mean:					0.76(2)	
$(8^+)$	$(10^+)$	290.4(5)	557.1(5)	1.7(2)	0.07(3)	0.07
	$(11^+)$	312.7(5)	603.3(5)	3.9(20)	0.05(15)	
Weighted mean:					0.07(3)	

In previous studies, the  $K^\pi = 4^-$  and  $5^+$  states were assigned to the  $\pi 5/2^+[402] \otimes \nu 3/2^-[512]$  and  $\pi 9/2^-[514] \otimes \nu 1/2^-[510]$  configurations, respectively [3, 7, 8, 14]. The weighted-mean experimental  $|g_K - g_R|$  values deduced in the present work,  $|g_K - g_R|_{\text{exp}} = 0.88(4)$  ( $K^\pi = 4^-$ ) and  $0.76(2)$  ( $K^\pi = 5^+$ ), are in good agreement with the predicted values of 0.93 and 0.73 for these two configurations. There is also good agreement between the experimental and predicted energies for these states, as shown in the comparison of Table II.

The  $K^\pi = (8^+)$  isomer was proposed to arise from the  $\pi 5/2^+[402] \otimes \nu 11/2^+[615]$  configuration [3, 7, 8, 14], based on the expected intrinsic states at low excitation energies in  $^{186}\text{Re}$ , as well as on theoretical predictions. The value  $|g_K - g_R| = 0.07(3)$  deduced in the present work is in good agreement with the value of 0.07 expected for this configuration. The alternative  $K^\pi = 8^+$ ,  $\pi 9/2^-[514] \otimes \nu 7/2^-[503]$  configuration is unlikely, since the predicted value of  $|g_K - g_R| = 0.61$  for this configuration differs significantly from the experimental value. The  $K^\pi = 8^+$ ,  $\pi 5/2^+[402] \otimes \nu 11/2^+[615]$  rotational band is also known in the neighboring odd-odd  $^{184}\text{Re}$  isotope [14]. Both bands have similar moments of inertia, as evident from Fig. 3, and  $|g_K - g_R|$  values are consistent with both arising from the same configuration.

The structure of the  $J^\pi = 10^+$  level is less certain. One possibility could be the four-quasiparticle  $\pi 5/2^+[402] \otimes \nu(1/2^-[510], 3/2^-[512], 11/2^+[615])$  configuration, which is predicted to be  $\sim 200$  keV above the observed level energy. Alternatively, a coupling of the  $K^\pi = 2^+$  vibrational state to the  $\pi 5/2^+[402] \otimes \nu 11/2^+[615]$  configuration could also be invoked. The  $K^\pi = 2^+$  bandheads are known at 767 keV and 633 keV in  $^{186}\text{Os}$  [4] and  $^{188}\text{Os}$  [27], respectively. Given the limited spectroscopic information available for the  $J^\pi = (11^+)$ , 1138.3-keV state, it is not

clear if it has an intrinsic or collective structure, and hence no configuration is assigned.

## V. SUMMARY

New  $\gamma$ -ray spectroscopy studies of the deformed, odd-odd  $^{186}\text{Re}$  nucleus were carried out using  $^{186}\text{W}(\text{d}, 2\text{n})$  reactions and the CAESAR (ANU) and CAGRA (Osaka University) multi-detector arrays. The rotational band associated with the long-lived,  $K^\pi = (8^+)$  isomer, as well as collective structures built upon the  $K^\pi = 4^-$  and  $5^+$  two-quasiparticle states, were established for the first time. Experimentally determined  $|g_K - g_R|$  values were deduced from measurements of in-band branching intensities, and a comparison of these values with theoretical predictions unambiguously supported the proposed configurations. Multi-quasiparticle blocking calculations, which included adjustment of the single-particle states near the proton and neutron Fermi surfaces, the Lipkin-Nogami pairing method, and the additional effect of the residual proton-neutron interactions, were carried out. Predicted intrinsic-state energies were found to be in good agreement with the experimental observations.

## VI. ACKNOWLEDGMENTS

This work was supported in part by the U.S. Department of Energy, Office of Science, Office of Nuclear Physics, under Contract No. DE-AC-06CH11357 (ANL), the Australian Research Council under projects DP0343027, DP0345844 and FT100100991, and the U.S. Army Research Laboratory under Cooperative Agreement W911NF-12-2-0019. Additional funding was provided by the Domestic Nuclear Detection Office of the

Department of Homeland Security. The authors gratefully acknowledge the help provided by the operations staffs at the ANU and RCNP accelerator facilities.

- 
- [1] F. G. Kondev, G. D. Dracoulis, and T. Kibédi, *At. Data Nucl. Data Tables* **103-104**, 50 (2015).
  - [2] G. D. Dracoulis, P. M. Walker, and F. G. Kondev, *Prog. Rep. Phys.* **79**, 076301 (2016).
  - [3] D. W. Seegmiller, M. Lindner, and R. A. Meyer, *Nucl. Phys.* **A185**, 94 (1972).
  - [4] C. M. Baglin, *Nucl. Data Sheets* **99**, 1 (2003).
  - [5] T. Hayakawa, T. Shizuma, T. Kajino, S. Chiba, N. Shinohara, T. Nakagawa, and T. Arima, *Astrophys. J.* **628**, 533 (2005).
  - [6] D. A. Matterns, A. G. Lerch, A. M. Hurst, L. Szentmiklósi, J. J. Carroll, B. Detwiler, Zs. Révay, J. W. McClory, S. R. McHale, R. B. Firestone, B. W. Sleaford, M. Krťička, and T. Belgya, *Phys. Rev. C* **93**, 054319 (2016).
  - [7] R. G. Lanier, R. K. Sheline, H. F. Mahlein, T. von Egidy, W. Kaiser, H. R. Koch, U. Gruber, B. P. K. Maier, O. W. B. Schult, D. W. Hafemeister, and E. B. Shera, *Phys. Rev.* **178**, 1919 (1969).
  - [8] J. Glatz, *Z. Phys.* **265**, 335 (1973).
  - [9] C. Wheldon, N. I. Ashwood, N. Curtis, M. Freer, T. Munoz-Britton, V. A. Ziman, T. Faestermann, H. F. Wirth, R. Hertenberger, R. Lutter, R. Gernhäuser, R. Krücken, and L. Maier, *J. Phys. G* **36**, 095102 (2009).
  - [10] D. A. Matterns, N. Fotiades, J. J. Carroll, C. J. Chiara, J. W. McClory, T. Kawano, R. O. Nelson, and M. Devlin, *Phys. Rev. C* **92**, 054304 (2015).
  - [11] D. C. Radford, *Nucl. Instrum. Methods Phys. Res. Sect. A* **361**, 297 (1995).
  - [12] T. Kibédi, T. W. Burrows, M. B. Trzhaskovskaya, P. M. Davidson, and C. W. Nestor, *Nucl. Instrum. Methods Phys. Res. Sect. A* **589**, 202 (2008).
  - [13] K. Brandi, R. Engelmann, V. Hepp, E. Kluge, H. Krehbiel, and U. Meyer-Berkhout, *Nucl. Phys.* **A59**, 33 (1964).
  - [14] C. Wheldon, G. D. Dracoulis, A. N. Wilson, P. M. Davidson, A. P. Byrne, D. M. Cullen, L. K. Pattison, S. V. Rigby, D. T. Scholes, G. Sletten, and R. Wood, *Nucl. Phys.* **A763**, 1 (2005).
  - [15] F. G. Kondev, G. D. Dracoulis, A. P. Byrne, T. Kibédi, and S. Bayer, *Nucl. Phys.* **A617**, 91 (1997).
  - [16] R. Bengtsson and I. Ragnarsson, *Nucl. Phys.* **A436**, 14 (1985).
  - [17] P. Möller, J. R. Nix, W. D. Myers, and W. J. Swiatecki, *At. Data Nucl. Data Tables* **59**, 185 (1995).
  - [18] S. C. Wu, *Nucl. Data Sheets* **106**, 619 (2005).
  - [19] M. Wang, G. Audi, A. H. Wapstra, F. G. Kondev, M. MacCormick, X. Xu, and B. Pfeiffer, *Chin. Phys. C* **36**, 1603 (2012).
  - [20] K. Jain, O. Burglin, G. D. Dracoulis, B. Fabricius, P. M. Walker, and N. Rowley, *Nucl. Phys.* **A591**, 61 (1995).
  - [21] F. G. Kondev, Ph.D. Thesis, Australian National University, 1996, unpublished.
  - [22] A. Bohr and B. R. Mottelson, *Nuclear Structure vol. 2*, World Scientific, River Edge, NJ, 1998.
  - [23] S. Buttgenbach, R. Dicke, G. Golz, and F. Traber, *Z. Phys. A* **302**, 281 (1981).
  - [24] M.L. Bissell, K.T. Flanagan, M.D. Gardner, M. Avgouleas, J. Billowes, P. Campbell, B. Cheal, T. Eronen, D.H. Forest, J. Huikari, A. Jokinen, I.D. Moore, A. Nieminen, H. Penttilä, S. Rinta-Antila, B. Tordoff, G. Tunge, and J. Äystö, *Phys. Lett. B* **645**, 330 (2007).
  - [25] S. Cwiok, J. Dudek, W. Nazarewicz, J. Skalski, and T. Werner, *Comput. Phys. Commun.* **46**, 379 (1987).
  - [26] P. Möller, A. J. Sierk, T. Ichikawa, and H. Sagawa, *At. Data Nucl. Data Tables* **109-110**, 1 (2016).
  - [27] B. Singh, *Nucl. Data Sheets* **95**, 387 (2002).